Supplemental Information for "Theory of hierarchically-organized neuronal oscillator dynamics that mediate rodent rhythmic whisking"

Supplemental Figure 1. Dynamics of the rate model for the pBötC-vIRt$^{\mathrm{ret}}$-vFMN circuit.

Time courses of $g^{\mathrm{rB}}g^{\mathrm{B}}$, M^{r}, a^{r}, M^{F} and a^{F} are plotted for the six cases by representing values of g^{rB}. The time traces are calculated using numerical simulations of the rate model, with $\Delta T_{\mathrm{pBötC}} = 70\,\mathrm{ms}$, $T_{\mathrm{pBötC}} = 700\,\mathrm{ms}$. The time constant τ_s is reduced to 0.1 ms to make the condition $\tau_s \ll \tau_{\mathrm{a}}^{\mathrm{r}}, \tau_{\mathrm{a}}^{\mathrm{F}}$, under which the rate-based analytical theory is developed, more accurate.

(A1) $g^{\mathrm{rB}} = 0.07\,\mathrm{mS/cm^2}$.

(A2) $g^{\mathrm{rB}} = 0.15\,\mathrm{mS/cm^2}$

(B1.1) $g^{\mathrm{rB}} = 0.32\,\mathrm{mS/cm^2}$.

(B1.2) $g^{\mathrm{rB}} = 0.4\,\mathrm{mS/cm^2}$.

(B2) $g^{\mathrm{rB}} = 0.55\,\mathrm{mS/cm^2}$.

(C) $g^{\mathrm{rB}} = 0.75\,\mathrm{mS/cm^2}$.

Supplemental Figure 2. Dynamical properties of circuits without pBötC input to the vIRt and $g_{\mathrm{intra}} = 0$.

(A) Schematic of the circuit. The dynamics are calculated for $g_{\mathrm{intra}} = 0$, $g^{\mathrm{r}}_{\mathrm{adapt}}$ = 7 mS/cm^2, $g^{\mathrm{F}}_{\mathrm{adapt}}$ = 0.3 mS/cm^2 and $I^{\mathrm{F}}_{\mathrm{ext}}$ = 3.1 μA/cm^2. The excitatory input is fixed at $I^{\mathrm{r}}_{\mathrm{ext}}$ = 20 μA/cm^2 and g_{inter} is varied for the data in panels B, D, F, H, and J. The conductane g_{inter} is fixed at 6 mS/cm^2 (black arrow in in panel J) with I_{ext} varying for the data in panels C, E, G, I, and K. Properties are computed using three modeling strategies, as in Figure 3F-G, and we use the same notation.

(B,C) The average spike rate $\langle M \rangle_i$. The rate model exhibits three dynamical regimes. For $0 \leq g_{\mathrm{inter}} \leq g_{\mathrm{tr}}$, the neuronal subpopulations are constantly spiking. For $g_{\mathrm{tr}} < g_{\mathrm{inter}} \leq g_{\mathrm{det}}$, the two subpopulation oscillate in a symmetric manner and are alternately active. The values of $\langle M \rangle_i$ for the vIRt$^{\mathrm{ret}}$ and vIRt$^{\mathrm{pro}}$ subpopulations are equal in the uniform and oscillatory states. For $g_{\mathrm{inter}} > g_{\mathrm{det}}$, one subpopulation is constantly active and the other one is silent. The values of g_{tr} and g_{det} are defined in the Star Methods. The regime $g_{\mathrm{tr}} \leq g_{\mathrm{inter}} \leq g_{\mathrm{det}}$ is denoted grey in panels B, D, F, H, J. The values of $\langle M \rangle_i$ for the two vIRt subpopulations, computed from simulations of the conductance-based model, are similar to those computed from the rate model for $g_{\mathrm{inter}} \leq g_{\mathrm{det}}$. As of g_{inter} increases beyond g_{det}, one subpopulation of conductance-based neurons becomes more active than the other. The less active subpopulation becomes silent at large values of g_{inter}. Therefore, the actual transition to the bistable state in the conductance-based model occurs for a g_{inter} value larger than the transition value for the rate model, g_{det}.

(D,E) The average whisking amplitude $< \theta^{\mathrm{amp}} >_t$. Analytical results are computed in panel D for the uniform and the bistable state.

(F,G) The whisking frequency $1/T_{\mathrm{vIRt}}$.

(H,I) The whisking set-point $< \theta^{\mathrm{set}} >_t$. Analytical results are computed in panel H for the uniform and the bistable state.

(J,K) The coefficient of variation $\langle \mathrm{CV}_2 \rangle_i$ calculated solely from the conductance-based equations.

Supplemental Figure S3. Effects of the onset time of pBötC activity on the amplitude of the subsequent whisk.

Values of the amplitude $\theta_1^{\rm amp}$ (Figure 7B) of vIRt$^{\rm ret}$ neurons are plotted as a function of $\Delta t_{\rm Bw,1}$. Each circle represents an amplitude of one whisk after the onset of pBötC activity. Parameters:

(A) $T_{\rm pBötC} = 250$ ms, $T_{\rm rand} = 150$ ms.

(B) $T_{\rm pBötC} = 200$ ms, $T_{\rm rand} = 70$ ms.

(C) $T_{\rm pBötC} = 250$ ms, $T_{\rm rand} = 70$ ms.

Explanation and relation to Figure 7F:

The difference $\Delta t_{\rm Bw,1} = t_{\rm B} - t_{\rm w,1}$ affects the amplitude of the following whisk, $\theta_1^{\rm amp}$ (Figure 7B). The onset of pBötC activity at time $t_{\rm B}$ initiates a new protraction. For $\Delta t_{\rm Bw,1} \ll T_{\rm vIRt}$, the vibrissae starts this new protraction at the beginning of the retraction phase, when it is already protracted (Figure 7B, top). As a result, the following $\theta_1^{\rm amp}$ is small. In contrast, when $\Delta t_{\rm Bw,1}$ is close to $T_{\rm vIRt}$ (here $T_{\rm vIRt} = 157\,{\rm ms}$), the vibrissae are already protracting just before $t_{\rm B}$, and the pBötC input enhances the protraction angle ((Figure 7B, bottom). If the pBötC onset is randomized, for example, when $T_{\rm rand} \sim T_{\rm vIRt}$, values of $\Delta t_{\rm Bw,1}$ are spread over almost the entire range from 0 to $T_{\rm vIRt}$, and $\theta_1^{\rm amp}$ values increase with $\Delta t_{\rm Bw,1}$ and eventually saturate (panel A). For smaller values of $T_{\rm rand}$, $\Delta t_{\rm Bw,1}$ values are restricted to a narrower interval of $\Delta t_{\rm Bw,1}$. For example, if $T_{\rm pBötC} \gtrsim T_{\rm vIRt}$, $t_{\rm Bw,1}$ is about $\Delta T_{\rm pBötC}$ after the last onset of pBötC activity, and $\Delta t_{\rm Bw,1}$ is between $T_{\rm pBötC} - \Delta T_{\rm pBötC} - T_{\rm rand}/2$ and $T_{\rm pBötC} - \Delta T_{\rm pBötC} + T_{\rm rand}/2$. Panel B depicts such a case, where $\Delta t_{\rm Bw,1}$ values are not near zero and $\theta_1^{\rm amp}$ is around its maximal value. Smaller $T_{\rm pBötC}$ entails smaller $\Delta t_{\rm Bw,1}$ and small $\theta_1^{\rm amp}$. For larger $T_{\rm pBötC}$ beyond that of panel B, intervening whisks appear, leading to the appearance of small $\Delta t_{\rm Bw,1}$ values that follow the peaks of these intervening whisks and that lead to small $\theta_1^{\rm amp}$ values (panel C). This means that as $f_{\rm pBötC} = 1/T_{\rm pBötC}$ decreases, the average $\theta_1^{\rm amp}$, $\langle \theta_1^{\rm amp} \rangle_t$, reaches a maximal value at about $T_{\rm pBötC} = T_{\rm vIRt}$ (Fig. 7F).

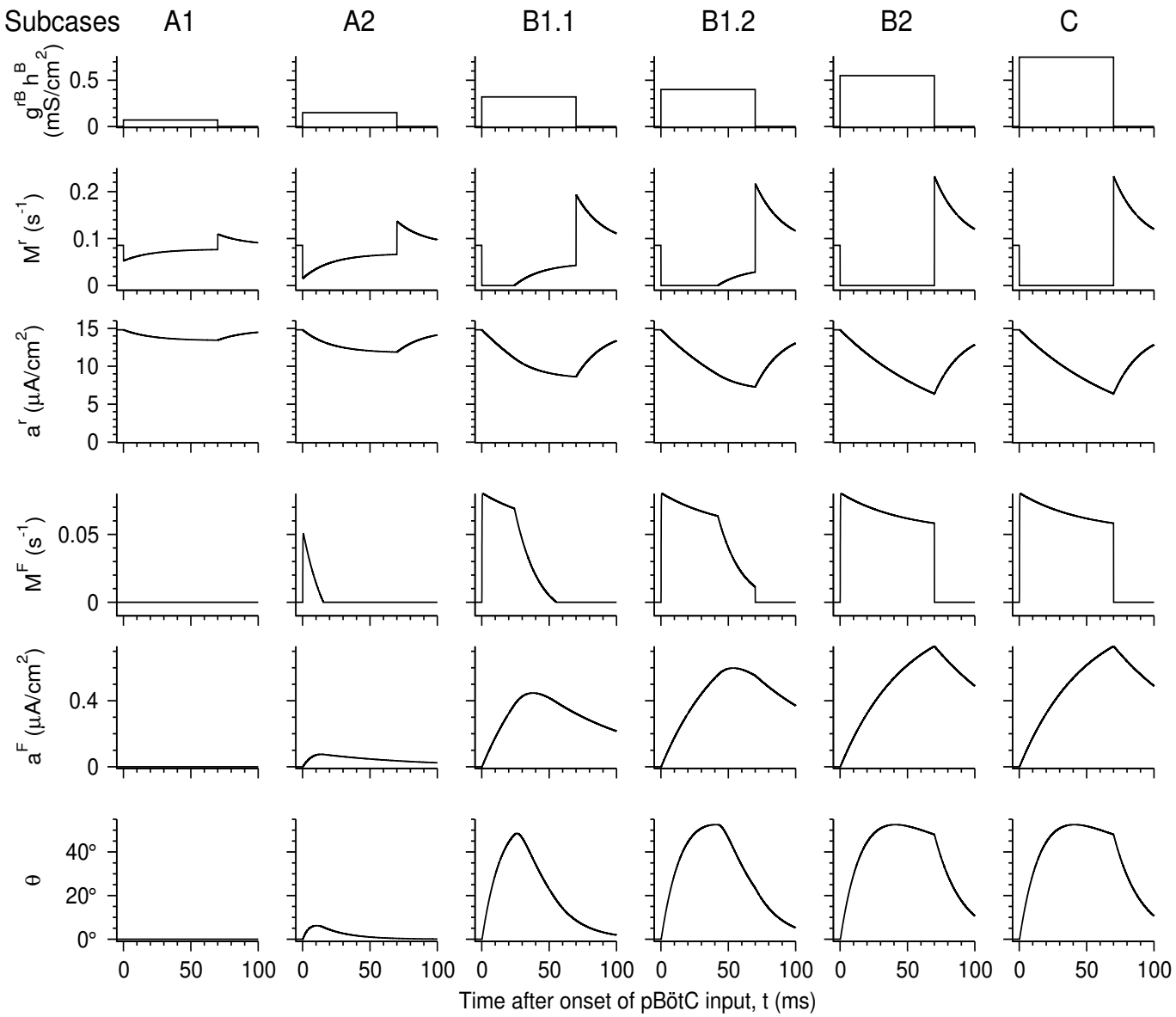

Supplementary Figure 1. Golomb et al.

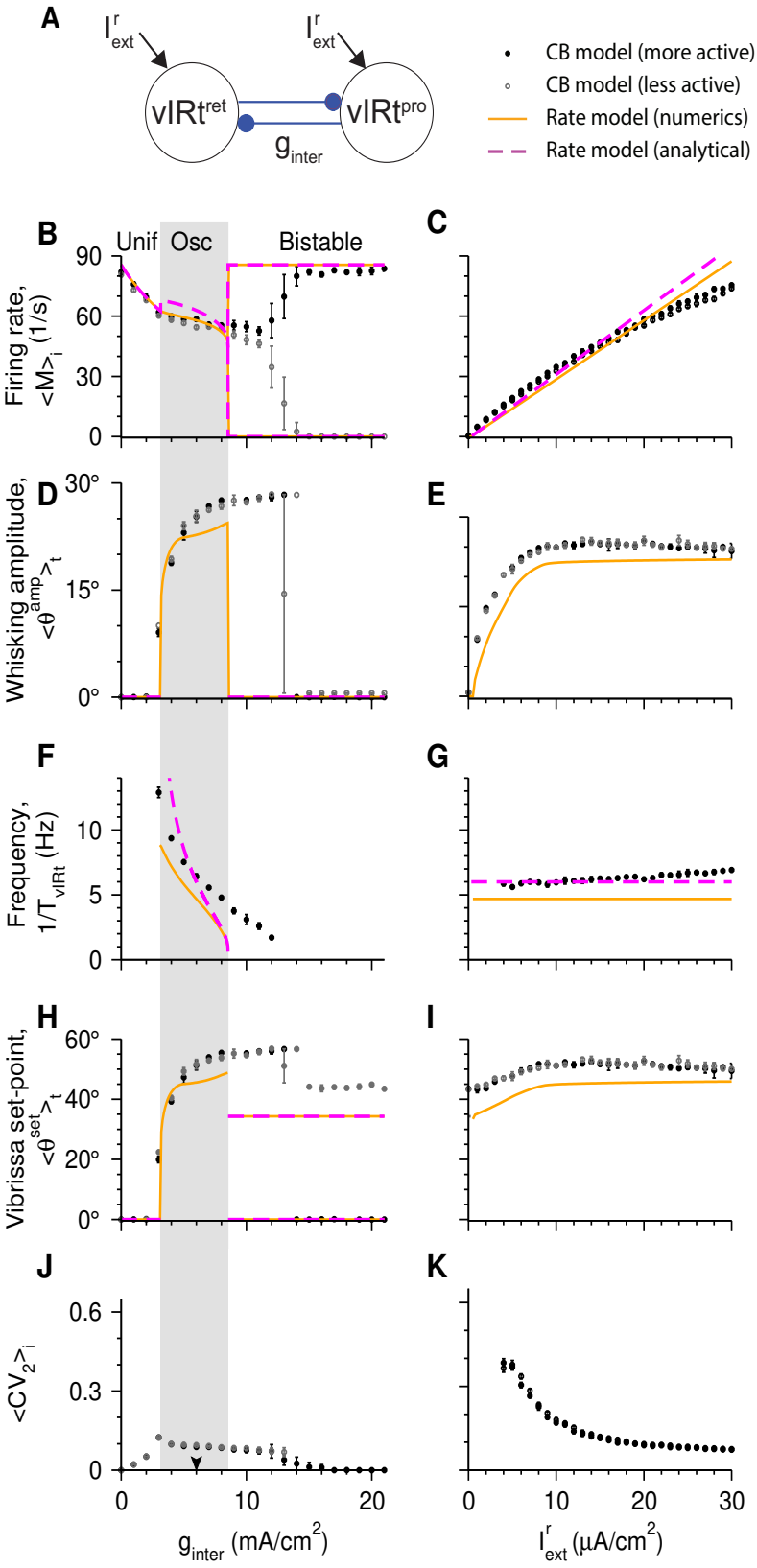

Supplementary Figure 2. Golomb et al.

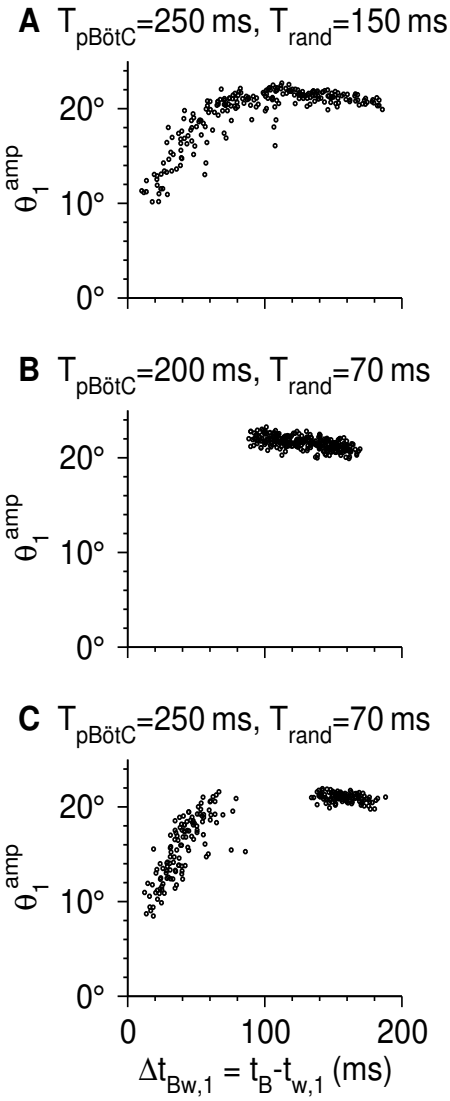

Supplementary Figure 3. Golomb et al.